JOURNAL OF SOLID STATE CHEMISTRY **123,** 371–377 (1996)
ARTICLE NO. 0191

Structures and Phase Transition of $Bi_2CdO_2[GeO_4]$

Robert E. Dinnebier[1] and Peter W. Stephens

Department of Physics, State University of New York at Stony Brook, New York 11974-3800

and

Stefan Wies and Walter Eysel

Mineralogisches Institut, Universität Heidelberg, 69120 Heidelberg, Germany

Received September 21, 1995; in revised form February 7, 1996; accepted February 8, 1996

The structure of $Bi_2CdO_2[GeO_4]$ was solved *ab initio* on the basis of laboratory and synchrotron X-ray powder data. The high temperature orthorhombic phase, stable at room temperature, crystallizes in *Pbcn* (60), $Z = 8$, $a = 10.4969(1)$ Å, $b = 10.0944(1)$ Å, $c = 5.60601(3)$ Å, and $V = 594.01(1)$ Å^3 with 14 refinable positional parameters. The structure consists of $[GeO_4]$ tetrahedra, strongly distorted trigonal $[CdO_6]$ prisms and irregular $[BiO_{4+2}]$ polyhedra. At low temperatures, the material undergoes a small distortion to monoclinic symmetry ($\gamma = 90.37°$ at 20 K).

I. INTRODUCTION

$Bi_2CdO_2[GeO_4]$ was obtained as a new ternary oxide during investigations of the system Bi_2O_3–CdO–GeO_2 (1–3). The orthorhombic unit cell data were determined by the Guinier technique with $a = 10.4969(1)$ Å, $b = 10.0944(1)$ Å, $c = 5.60601(3)$ Å. The only possible space group derived from powder extinctions is *Pbcn.* It appeared to be worthwhile to attempt a structure determination because of the variable coordination chemistry of Bi^{3+} with its lone electron pair. In addition, Cd^{2+} exhibits an unusual variety of CdO_n polyhedra.

DSC investigations resulted in a melting point at 790°C on heating. Attempts to grow single crystals from a melt with the ideal composition failed, indicating an incongruent melting point. By hydrothermal treatment of $Bi_2CdO_2[GeO_4]$ powder at 2 kbar and 630 or 750°C, turquoise, cube-like crystals up to 0.2 mm in diameter were obtained. Unfortunately, these turned out to be multiply twinned. Therefore it was decided to try an *ab initio* structure determination from a powder sample. A preliminary account of these results was given in (4).

[1] Present address: Lehrstuhl für Kristallographie, University of Bayreuth, 95440 Bayreuth, Germany.

II. EXPERIMENTAL

Powder samples of $Bi_2CdO_2[GeO_4]$ were prepared from a stoichiometric mixture of Bi_2O_3 (Ventron, ultrapure), CdO (Ventron, 99.9%), and GeO_2 (Ventron, ultrapure). The mixture was melted at 1000°C in an open gold crucible for some minutes and subsequently annealed at 750°C for 3 days (3). Small traces of $Cd_{0.2}Bi_{1.8}GeO_5$ were present (5).

The XRPD data for the structure determination were first collected at room temperature at the SUNY X3B1 beamline at the National Synchrotron Light Source, Brookhaven National Laboratory. The sample was prepared by the side loading technique using a flat quartz single crystal $(10\bar{1}1)$ sample holder. X-rays of wavelength approximately 1.15 Å were selected by a double Si(111) monochromator. The diffracted beam was analyzed by reflection from a Ge(111) crystal before a NaI scintillation detector. In this parallel beam configuration, the resolution is determined by the analyzer crystal instead of by slits. Data were taken for 2 s at each 2Θ step of 0.005° from 8° to 88° for the high temperature phase (at 298 K) and for 3 s at each 2Θ step of 0.005° from 7° to 87° for the low temperature phase (at 20 K). All data were normalized for storage ring current decay by an ionization chamber monitor. Low angle diffraction peaks from this sample had a width of 0.032° FWHM in 2Θ, significantly broader than the resolution of the spectrometer. The pathway from raw data to the refined structure was straightforward and details of each step are given in Section III.

To evalute the possibility of a distortion at low temperature, the sample was cooled to 20 K in a closed cycle cryostat. From the pattern collected, a monoclinic distortion was eivident. Lattice parameters at intermediate temperatures were also determined from scans over a limited range of 2Θ.

0022-4596/96 $18.00

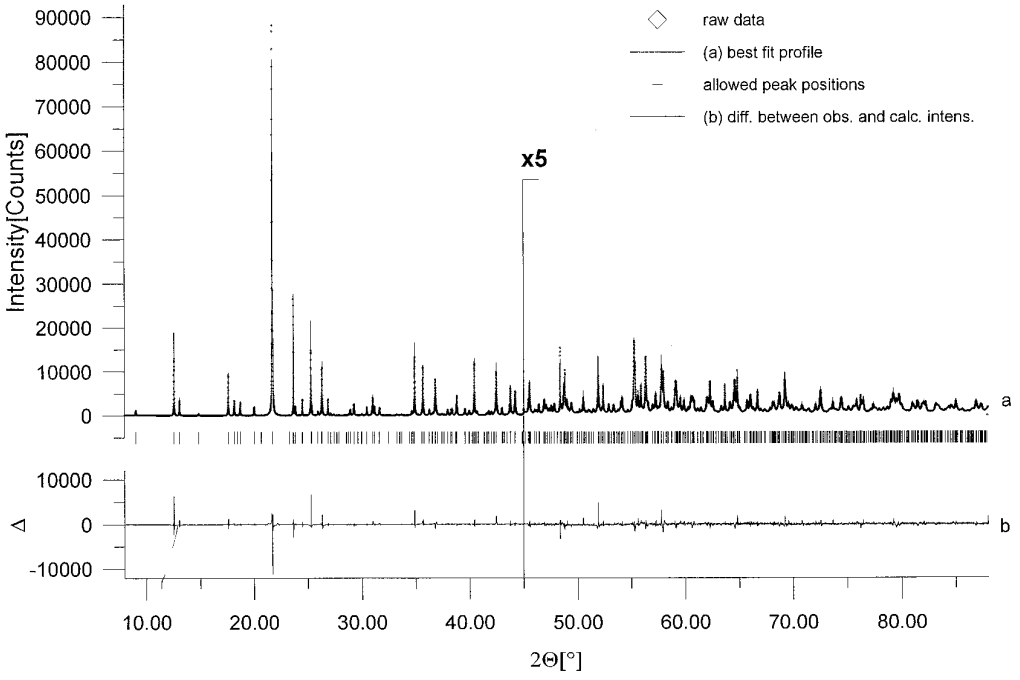

FIG. 1. Rietveld plot of the high temperature phase of $Bi_2CdO_2[GeO_4]$, at ambient temperature (λ = 1.14853(2) Å).

III. RESULTS

At the beginning of the structure solution the profile matching and Rietveld program FULLPROF (6) was used to confirm the space group and to extract about 256 integrated intensities up to $2\Theta = 65°$ from the room temperature phase. Due to the highly resolved peaks over the entire angular range, direct methods appeared favorable for a structure solution. Therefore the extracted intensities were used as an input for the direct method program SIRPOW.92 (7). The program with its default settings could find the positions of the Bi and Cd atoms automatically. Because these atoms are so much heavier than the remaining Ge and O, the rest of the structure could be solved by the difference Fourier method.

TABLE 1
Positional Parameters for the High Temperature Phase of $Bi_2CdO_2[GeO_4]$ in *Pbcn*

Atom	x/a	y/b	z/c	Site symm.	$U_i/U_e * 100$
Bi	0.2598(1)	0.1092(1)	0.2826(1)	1	0.47(4)
Cd	0.5	0.3871(3)	0.25	.2.	0.78(9)
Ge	0.0	0.3486(3)	0.25	.2.	0.3(2)
O1	−0.078(1)	0.249(1)	0.034(2)	1	0.0(1)
O2	0.126(1)	0.448(1)	0.128(2)	1	0.0(1)
O3	0.150(1)	0.026(1)	−0.015(2)	1	0.0(1)

Preliminary Rietveld refinements (8) using the GSAS program system (9) without Ge and O atoms converged with the positions of the heavy atoms. Due to the fact that these fits appeared very poorly in terms of intensitites (weighted profile R factor of 53.9%) it was necessary to fix the profile parameters to the values determined by profile matching.

After calculating difference Fourier sections perpendicular to the c axis, the Ge atoms appeared. Consecutive Rietveld refinement (weighted profile R factor of 35.5%) and difference Fourier calculation showed the positions of the three independent O atoms. The final Rietveld plot (weighted profile R factor of 12.8%, profile R factor of 9.6%), with 553 reflections, is given in Fig. 1, with the results listed in Table 1. Since it was not possible to refine the temperature factors fo the three oxygens independently in the presence of the heavy Bi and Cd atoms, they had to be constrained to be equal, at which point they converged to a value close to zero. During the refinement of both phases, soft constraints were used for the Ge–O distances in the tetrahedron (Ge–O) distance of 1.78 Å).

The sample shows strongly anisotropic peak broadening. A plot of the widths of selected, well-resolved peaks vs 2Θ in Fig. 2 shows that they vary by as much as a factor of 2.5 at a given 2Θ. If this anisotropy is not taken into account, the weighted profile R factors of the profile fit an the refined structure are quite poor, 16.7%. The best agreement between model and data was obtained using

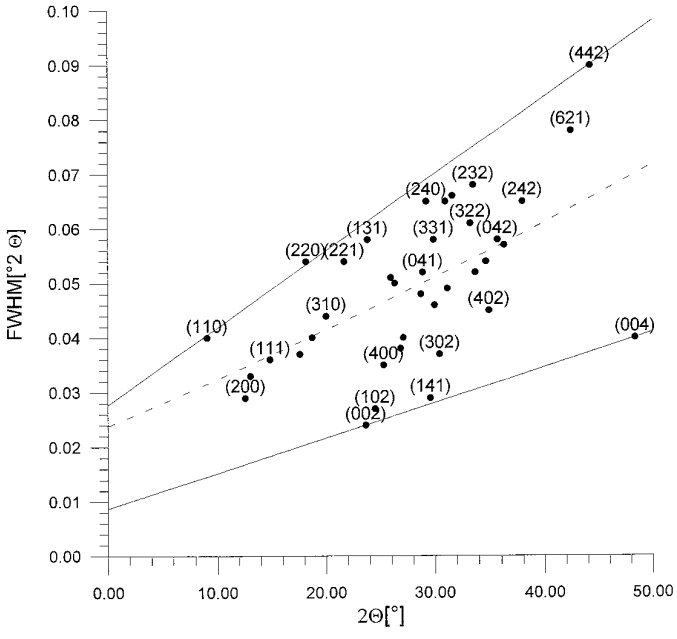

FIG. 2. Distribution of selected peak widths of the high temperature phase of $Bi_2CdO_2[GeO_4]$ in the range from 0° to 50° 2Θ showing strong anisotropical strain broadening along [110]. The dashed line marks a least squares fit of a second degree polynomial to all displayed full widths at half maximum, whereas the outer lines are linear fits along the strain direction and perpendicular to it.

the anisotropic strain model of the program GSAS. In this model, the Lorentzian width γ is a function of the Bragg angle 2Θ and the angle Φ between the diffraction vector and the strain axis, here [110], in terms of four parameters, X, X_e, Y, and Y_e as

$$\gamma = \frac{X + X_e \cos \Phi}{\cos \Theta} + (Y + Y_e \cos \Phi) \tan \Theta.$$

Even this model gives an imperfect fit to the data. The values of R_{wp} for profile extraction and structural refinement remain equal, 12.8%, indicating that most of the discrepancies of the Rietveld fit to the data are due to the lineshape parameters (fitting lineshapes to data) rather than the structural model (integrated intensities). The low value of the Bragg R factor based on the integrated intensities, 3.2%, confirms the validity of the structural model in the face of the lineshape distortion. It is interesting to note that SIRPOW.92 was also able to find the complete structure (all atoms) ''from scratch,'' using the anisotropic strain model and all the extracted intensities up to 88° 2Θ.

The profile collected at 20 K is shown in Fig. 3. In comparison with the room temperature data set, the (hkl) and ($hk0$) peaks have split, whereas ($0kl$) and ($h0l$) remain as single peaks. This implies a small monoclinic distortion between the a and b axes of the room temperature phase. The refined lattice parameters at 20 K are a = 10.4795(1)

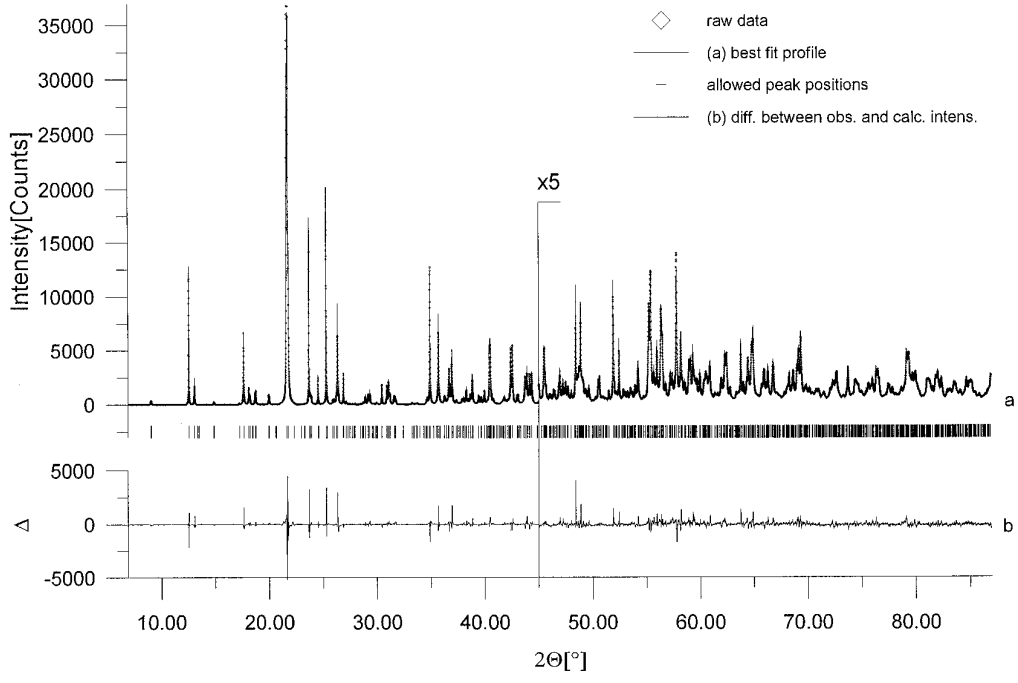

FIG. 3. Rietveld plot of $Bi_2CdO_2[GeO_4]$ at 20 K (λ = 1.14795(2) Å).

TABLE 2
Positional Parameters for the Low Temperature Phase of $Bi_2CdO_2[GeO_4]$ in $P1\ 2_1/n\ 1$

Atom	x/a	y/b	z/c	Site symm.	$U_i/U_e * 100$
Bi1	0.2624(1)	0.2838(5)	0.1092(1)	1	0.44(5)
Bi2	−0.2555(1)	0.2159(5)	0.1102(1)	1	0.56(5)
Cd	0.4997(2)	0.2498(8)	0.3850(2)	1	0.25(5)
Ge	0.0017(4)	0.254(1)	0.3503(3)	1	0.23(10)
O1	−0.063(2)	0.037(2)	0.246(1)	1	0.6(2)
O2	0.069(2)	0.482(2)	0.257(2)	1	0.6(2)
O3	0.114(1)	0.125(3)	0.457(1)	1	0.6(2)
O4	−0.119(1)	0.372(3)	0.445(1)	1	0.6(2)
O5	0.142(2)	−0.012(3)	0.025(2)	1	0.6(2)
O6	−0.146(2)	0.506(3)	0.035(2)	1	0.6(2)

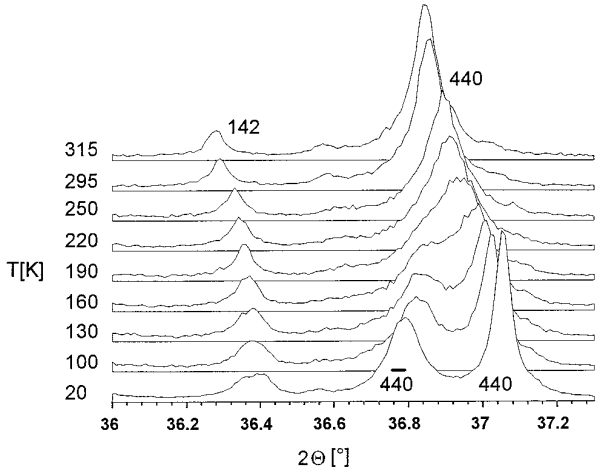

FIG. 4. Part of the powder pattern of $Bi_2CdO_2[GeO_4]$, showing the splitting of the reflections 142 and 440 as a function of temperature during heating.

Å, b = 10.0665(1) Å, c = 5.5891(1) Å, γ = 90.377(1)°, and V = 589.58(1) A^3.

The only suitable monoclinic subgroup of *Pbcn* is $P11\ 2_1/n$.[2] The lower symmetry of the monoclinic phase is achieved by removing the Cd and Ge atoms from special positions, and by doubling the number of independent Bi and O atoms. As a starting point for structural refinement, the fractional coordinates from the high temperature phase were transformed toward $P1\ 2_1/n\ 1$, since the computer program required b to be the unique axis. Using anisotropic peak widths (broadening axis (001) in $P_1\ 2_1/n\ 1$) for the refinement shown in Fig. 3, we obtained a fit of equal quality to the high temperature phase: R_{wp} = 12.0% for the leBail extraction, R_p = 9.9% R_{wp} = 13.0%, and R_{Bragg} = 3.1% for the Rietveld refinement. The number of reflections increased to 1066. The refinement produces very small shifts of all of the atoms (Table 2). As in the high temperature phase, the thermal parameters of O were constrained to be equal. A more rigorous approach using direct methods independently leads to exactly the same result for the positions of the metal atoms.

The phase transition between the monoclinic and the orthorhombic phases was studied by collecting partial X-ray patterns at various temperatures. The region of the orthorhombic (142) and (440) reflections is shown in Fig. 4. Lattice parameters, derived from data $34.3 < 2\Theta < 39.3$ are plotted in Fig. 5. It is interesting to note that the monoclinic distortion has not completely disappeared at 315 K, indicating some hysteresis in the transition. After annealing the sample

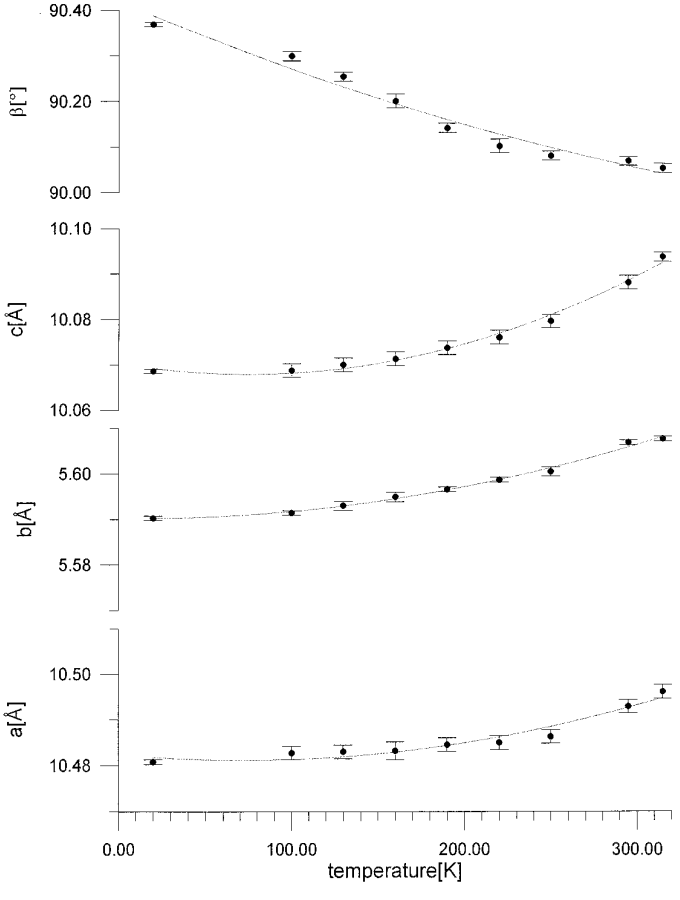

FIG. 5. Lattice parameters as a function of temperature for $Bi_2CdO_2[GeO_4]$ during heating. The exact orthorhombic angle of 90° could not be reached at 315 K.

[2] The standard setting of this space group is $P2_1/c$, and the transformation from unit cell axes (a, b, c) of $P11\ 2_1/n$ to (a', b', c') of $P1\ 2_1/c\ 1$ is $\begin{pmatrix} a' \\ b' \\ c' \end{pmatrix} = \begin{pmatrix} 1 & 0 & -1 \\ 0 & 0 & -1 \\ 0 & 1 & 0 \end{pmatrix} \begin{pmatrix} a \\ b \\ c \end{pmatrix}$. The lattice parameters of the unit cell of the low temperature phase in the standard setting are a' = 10.4794 Å, b' = 5.5891 Å, c' = 14.4833 Å, β' = 135.970°.

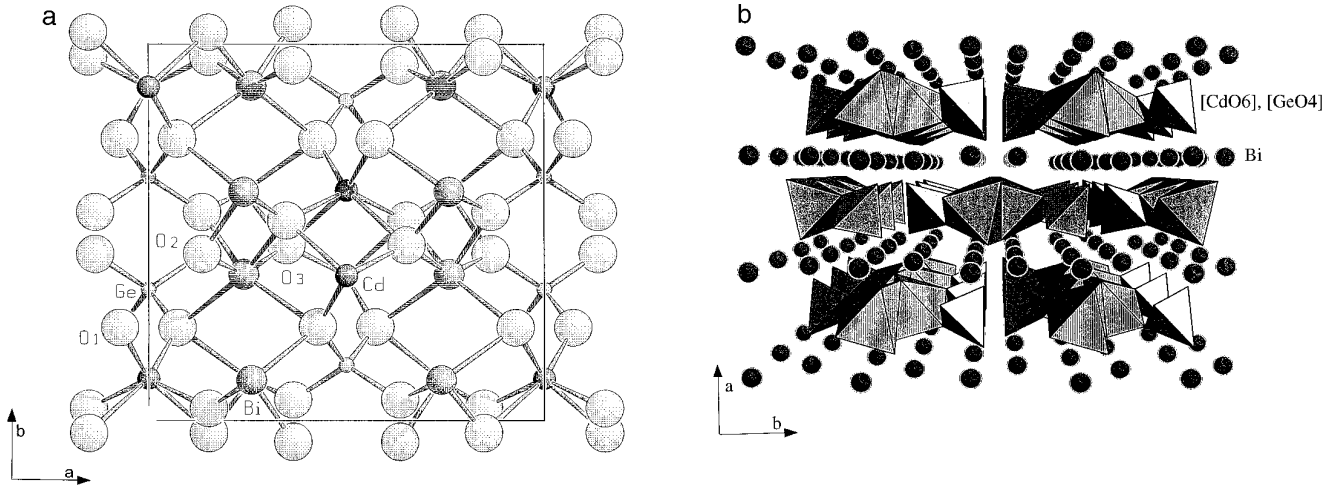

FIG. 6. (a) Stick and ball plot of the high temperature phase of $Bi_2CdO_2[GeO_4]$ ⊥ to *c* axis. Drawn with the program SCHAKAL (11). (b) Perspective view of the high temperature phase of $Bi_2CdO_2[GeO_4]$ ⊥ to *c* axis. The alternating cation sheets of Bi and (Cd + Ge) are visible. The $[GeO_4]$ and $[CdO_6]$ polyhedra are drawn.

at 600°C for several hours and measuring it again at room temperature, the monoclinic distortion was not visible. The monoclinic angle closely approaches 90° (Fig. 5) on approaching the transition temperature, suggesting a second-order type of transition. However, there is a clear hysteresis in the orthorhombic/monoclinic fractions, showing this phase transition to be first order.

In view of the fact that the as-prepared sample at 298 K is close to a structural distortion, it is tempting to suppose that this is the origin of the diffraction peak anisotropic broadening in the high temperature phase. A small shift of the angle between orthorhombic *a* and *b* axes would especially broaden (*hk*0) peaks with *h* close to *k*, but leave the (*h*0*l*) and (0*kl*) peaks sharp. Inspection of Fig. 2 shows that the former is observed but the latter is not; note especially the (402) and (042) peak widths, respectively 30% and 60% wider than the (interpolated) minimum peak width in that range of 2Θ. Accordingly, we must conclude that the distribution of microstrain in the orthorhombic crystals is not simply related to the incipient monoclinic distortion.

IV. DISCUSSION OF THE STRUCTURE

The structure of orthorhombic $Bi_2CdO_2[GeO_4]$ is illustrated in Fig. 6. It contains three types of anion polyhedra. The bond lengths and angles are given in Tables 3–5.

Germanium is coordinated by four oxygens (O1 + O2), in the form of an irregular tetrahedron, with values given in Table 3. The tetrahedra are deformed to orthorhombic bisphenoids with differing bond angles. The third oxygen in the structure (O3) is not bonded to the Ge tetrahedron.

Cadmium is coordinated by six oxygens which form a highly distorted trigonal prism with three different bond lengths and nine different bonding angles (Fig. 7a, Table 4). The roof-like coordination is very similar to that found in Cd_2SiO_4 (10). Every $[CdO_6]$ polyhedron shares two edges (O3–O3) with two neighboring $[CdO_6]$ polyhedra and the two corners of the roof ridge (O1–O1) with corners of two $[GeO_4]$ tetrahedra.

Bismuth has an irregular 4 + 2 coordination. Four oxygens form the basis of a distorted $[BiO_4]$ pyramid. The

TABLE 3
Distances and Angles for the $[GeO_4]$ Tetrahedron in $Bi_2CdO_2[GeO_4]$

Atoms of HT phase		Distances (Å)	Atoms of LT phase	Distances (Å)
Ge–O2	(2×)	1.77(1)	Ge–O1	1.74(1)
Ge–O1	(2×)	1.80(1)	Ge–O2	1.74(1)
			Ge–O3	1.75(1)
			Ge–O4	1.73(1)
Median		1.79	Median	1.74
Literature[a]		1.79	Literature[a]	1.79
Atoms of HT phase		Angles (°)	Atoms of LT phase	Angles (°)
O1–Ge–O1′		110.8(6)	O1–Ge–O2	110.3(7)
O2–Ge–O1	(2×)	113.4(4)	O1–Ge–O3	110.1(9)
O2–Ge–O1	(2×)	103.8(4)	O1–Ge–O4	108.3(8)
O2–Ge–O2′		111.9(5)	O2–Ge–O3	111.3(8)
			O2–Ge–O4	108.7(9)
			O3–Ge–O4	108.0(6)
Median		109.5	Median	109.5

[a] Literature values are on the basis of effective ionic radii after Shannon (12) in the specific coordination.

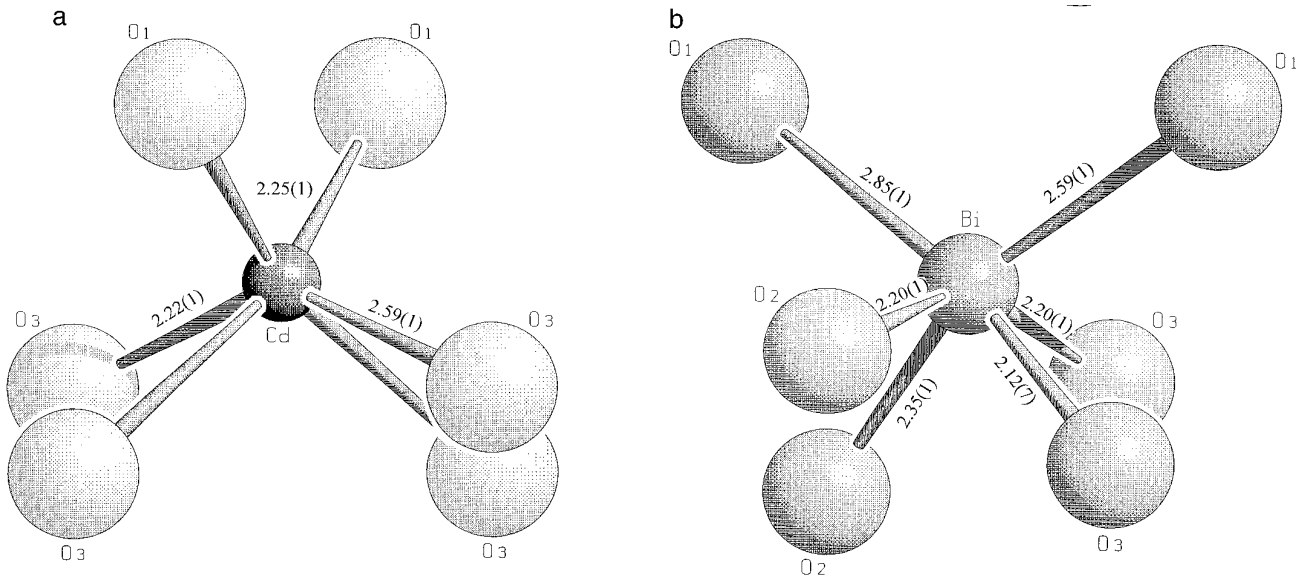

FIG. 7. (a) $[CdO_6]$ polyhedra of the high temperature phase of $Bi_2CdO_2[GeO_4]$. (b) $[BiO_{4+2}]$ polyhedra of the high temperature phase of $Bi_2CdO_2[GeO_4]$.

pyramids are connected by common oxygen edges in the *c*-direction (Fig. 7b, Table 5). The lone electron pairs of the Bi^{3+} ion point alternatingly up and down along *b* (Fig. 6a), pushing the two more distant oxygens O1 aside. As pointed out before, the low temperature structure deviates from the high temperature form only by minimal atomic shifts, listed in Tables 3–5. A remarkable feature of this structure is a chemical ordering of the metal atoms. They are segregated into sheets perpendicular to the *a* axis containing either Bi or Cd and Ge. This opens the possibility for the structure to have low-dimensional electron properties, based on relatively short Bi–Bi distances within a

TABLE 4
Distances and Selected Angles for the $[CdO_6]$ Polyhedron in $Bi_2CdO_2[GeO_4]$

Atoms of HT phase		Distances (Å)	Atoms of LT phase	Distances (Å)
Cd–O1	(2×)	2.25(1)	Cd–O1	2.19(1)
Cd–O2	(2×)	2.23(1)	Cd–O2	2.19(1)
Cd–O3	(2×)	2.58(1)	$Cd–O5_I$	2.20(2)
			$Cd–O5_{II}$	2.52(2)
			$Cd–O6_I$	2.21(2)
			$Cd–O6_{II}$	2.60(2)
Median		2.35	Median	2.32
Literature[a]		2.35	Literature[a]	2.35
Atoms of HT phase		Angles (°)	Atoms of LT phase	Angles (°)
O1–Cd–O1′		105.0(4)	O1–Cd–O2	101.9(6)
O1–Cd–O2	(2×)	94.4(3)	O1–Cd–O5	90.9(6)
O1–Cd–O2′	(2×)	113.6(3)	O1–Cd–O6	117.5(6)
O2–Cd–O3′		134.0(4)	O2–Cd–O5	117.7(6)
			O2–Cd–O6	92.5(6)
			O5–Cd–O6	133.9(5)
Median		109.1	Median	109.1

[a] Literature values are on the basis of effective ionic radii after Shannon (12) in the specific coordination.

TABLE 5
Distances and Selected Angles for the $[BiO_{4+2}]$ Polyhedron in $Bi_2CdO_2[GeO_4]$

Atoms of HT phase	Distances (Å)	Atoms of LT phase		Distances (Å)	
Bi–O1	2.85(1)	Bi1–O2	Bi2–O1	2.76(2)	2.63(2)
Bi–O1′	2.59(1)	Bi1–O2′	Bi2–O2	2.79(2)	3.00(2)
Bi–O2	2.20(1)	Bi1–O3	Bi2–O3	2.41(2)	2.24(1)
Bi–O2′	2.35(1)	Bi1–O4	Bi2–O4	2.25(1)	2.40(2)
Bi–O3	2.19(1)	Bi1–O5	Bi2–O5	2.25(2)	2.14(2)
Bi–O3′	2.12(7)	Bi1–O6	Bi2–O6	2.22(2)	2.13(2)
Median	2.38	Median		2.45	2.42
Literature[a]	2.38	Literature[a]		2.38	2.38
Atoms of HT phase	Angles (°)	Atoms of LT phase		Angles (°)	
O2–Bi–O2′	82.2(2)	O3–Bi1–O4,	O3–Bi1–O4	78.4(6),	80.0(6)
O2–Bi–O3	72.8(3)	O3–Bi1–O5,	O3–Bi1–O5	141.4(6),	96.7(6)
O2–Bi–O3′	91.6(3)	O3–Bi1–O6,	O3–Bi1–O6	72.1(6),	77.2(7)
O2–Bi–O3′	143.2(2)	O4–Bi1–O5,	O4–Bi1–O5	75.4(6),	74.4(6)
O2–Bi–O3	71.1(3)	O4–Bi1–O6,	O4–Bi1–O6	91.6(6),	145.5(6)
O3–Bi–O3′	82.8(2)	O5–Bi1–O6,	O5–Bi1–O6	80.7(6),	82.8(7)
Median	90.6	Median		89.9	92.8

[a] Literature values are on the basis of effective ionic radii after Shannon (12) in the specific coordination.

sheet, and a large Bi separation between the sheets. The small size of the distortions and relatively large uncertainties for the atomic coordinates as obtained from Rietveld refinements precludes the conclusion that the monoclinic distortion is due to such interactions.

ACKNOWLEDGMENTS

Research was carried out in part at the National Synchrotron Light Source at Brookhaven National Laboratory, which is supported by the U.S. Department of Energy, Division of Materials Sciences and Division of Chemical Sciences. The SUNY X3 beamline at NSLS is supported by the Division of Basic Energy Sciences of the U.S. Department of Energy under Grant DEFG-0286-ER-4531. Research at the University of Heidelberg was supported in part by the Deutsche Forschungsgemeinschaft and by the International Centre for Diffraction Data. PWS was supported by the NSF under Grant DMR-92-02529. Special thanks to Gerhard Hermeler from the University of Kiel (Germany), who suggested the phase transition due to crystallographic considerations.

REFERENCES

1. S. Wies, "Crystal Chemistry of the System Bi_2O_3-CdO-GeO_2." Ph.D. Thesis, in German, Heidelberger Geowissenschaftliche Abhandlungen, Vol. 65, ISBN 3-89257-064-7, 1993.
2. S. Wies and W. Eysel, ICDD-PDF, pattern No 41-406, 1991.
3. S. Wies and W. Eysel, *Powder Diff.*, in press (1996).
4. R. E. Dinnebier, P. W. Stephens, S. Wies, and W. Eysel, "Collected Abstracts, International Conference Powder Diffraction and Crystal Chemistry, June 20–23, 1994, St. Petersburg, Russia," p. 152–153, 1994.
5. Sussieck-Fornefeld and T. Gauder, ICDD-PF, pattern No 39-1258, 1989.
6. J. Rodriguez-Carvajal, "FULLPROF: A Program for Rietveld Refinement and Pattern Matching Analysis, Abstracts of the Satellite Meeting on Powder Diffraction of the XV Congress of the IUCr, Toulouse, France," p. 127, 1990.
7. G. Cascarano, L. Favia, and C. Giacovazzo, *J. Appl. Crystallogr.* **25,** 310 (1992).
8. H. M. Rietveld, *J. Appl. Crystallogr.* **2,** 65 (1969).
9. R. B. von Dreele and A. C. Larson, "General Structure Analysis System." Los Alamos National Laboratory Report LAUR 86-748, 1990.
10. R. E. Dinnebier "GUFI ein Programmsystem zur Messung und Auswertung von Roentgen-Beugungsaufnahmen an Pulvern." Dissertation, Min.-Petr. Inst., Universität Heidelberg, Heidelberger Geowiss. Abh., Vol. 68, ISBN 3-89257-067-1, 1993.
11. E. Keller, "SCHAKAL 1986: A Fortran Program for the Graphic Representation of Molecular and Crystallographic Models." Kristallographisches Institut der Universität Freiburg, Germany, 1986.
12. R. D. Shannon, *Acta Crystallogr. A* **32,** 751 (1976).